

# Topology preserving alternating sequential filter for smoothing 2D and 3D objects

Michel Couprie<sup>(a,b)</sup> and Gilles Bertrand<sup>(a,b)</sup>

(a) Laboratoire A<sup>2</sup>SI, ESIEE Cité Descartes B.P. 99, 93162 Noisy-Le-Grand Cedex France

(b) Institut Gaspard Monge, Unité Mixte de Recherche CNRS-UMLV-ESIEE UMR 8049

e-mail: m.couprie@esiee.fr, g.bertrand@esiee.fr; url: www.esiee.fr/a2si

## ABSTRACT

We introduce the homotopic alternating sequential filter as a new method for smoothing 2D and 3D objects in binary images. Unlike existing methods, our method offers a strict guarantee of topology preservation. This property is ensured by the exclusive use of homotopic transformations defined in the framework of digital topology. Smoothness is obtained by the use of morphological openings and closings by metric discs or balls of increasing radius, in the manner of an alternating sequential filter. The homotopic alternating sequential filter operates both on the object and on the background, in an equilibrated way. It takes an original image  $X$  and a control image  $C$  as input, and smoothes  $X$  “as much as possible” while respecting the topology of  $X$  and geometrical constraints implicitly represented by  $C$ . Based on this filter, we introduce a general smoothing procedure with a single parameter which allows to control the degree of smoothing. Furthermore, the result of this procedure presents small variations in response to small variations of the parameter value. We also propose a method with no parameter for smoothing zoomed binary images in 2D or 3D while preserving topology.

**Keywords:** Shape smoothing, digital topology, homotopy, mathematical morphology, alternating sequential filters.

## 1. INTRODUCTION

Shape smoothing plays an important role in image processing and pattern recognition. For example, the analysis or recognition of a shape is often perturbed by noise, thus the smoothing of object boundaries is a necessary pre-processing step. Also, when zooming or warping binary digital images, one obtains a crenelated result that must be smoothed for better visualization. The smoothing procedure can also be used to extract some shape characteristics: by making the difference between the original and the smoothed object, salient or carved parts can be detected and measured.

Many different approaches have been proposed for smoothing shapes:

- Ad hoc transformation rules applied to chain-coded object boundaries (2D only).<sup>1</sup>
- Morphological filtering applied directly to the shape.<sup>2</sup>
- Morphological filtering applied to a curvature plot of the object’s contour (2D only).<sup>3</sup>
- Filtering of the medial axis.<sup>4</sup>
- Filtering of a multiple scale boundary representation (2D morphological scale space).<sup>5</sup>
- Linear filtering. The most popular algorithm to perform linear filtering is the Laplacian smoothing (well suited to 2D-vector or 3D-mesh representations).<sup>6-9</sup>
- Diffusion equations: partial differential equations, similar to the classical heat equation, are used to model the evolution of a curve or a surface in space-time.<sup>10,11</sup>

In all previous works, it was always assumed that the shape to be smoothed is a single object, in other words, its boundary is a simple closed curve (in 2D) or surface (in 3D). What happens if we want to apply the smoothing to a whole scene composed of several objects? If we apply any of the proposed schemes to each object independently and then merge the results, there is no guarantee that the images of two disjoint objects will be disjoint. More generally, little attention has been paid to global topological properties of smoothing procedures. Even when applied to a single object, there is no formal proof that known smoothing schemes preserve the object’s topological characteristics (number of connected components and cavities, number of tunnels in 3D), with the remarkable exception of a result concerning the evolution of a 2D plane curve under the heat equation which has been proved to shrink towards one point.<sup>12</sup>

We introduce a new method for smoothing 2D and 3D objects in binary images while preserving topology. Here, objects are defined as sets of grid points, and topology preservation is ensured by the exclusive use of homotopic transformations defined in the framework of digital topology.<sup>13</sup> Smoothness is obtained by the use of morphological openings and closings by metric

discs or balls of increasing radius, in the manner of alternating sequential filters.<sup>14,15</sup> All these morphological filters do not preserve topology, this is why we introduce new operators: homotopic cutting and homotopic filling, which combine a filtering effect with the guarantee of topology preservation. The homotopic alternating sequential filter is a composition of homotopic cuttings and fillings by balls of increasing radius. It takes an original image  $X$  and a control image  $C$  as input, and smoothes  $X$  “as much as possible” while respecting the topology of  $X$  and geometrical constraints implicitly represented by  $C$ . Based on this filter, we introduce a general smoothing procedure with a single parameter which allows to control the degree of smoothing. Furthermore, the result of this procedure presents small variations in response to small variations of the parameter value. We also propose a method with no parameter for smoothing zoomed binary images in 2D or 3D while preserving topology.

## 2. BASIC NOTIONS OF MATHEMATICAL MORPHOLOGY

In this section, we recall some basic notions of mathematical morphology for binary images,<sup>16,15</sup> and the definition of alternating sequential filters.<sup>14</sup> For the sake of simplicity, we restrict ourselves to the minimal set of notions that will be useful for our purpose. In particular, we consider only morphological operators based on structuring elements which are balls in the sense of the Euclidean distance, in order to obtain the desired smoothing effect.

We denote by  $\mathbb{Z}$  the set of relative integers, and by  $E$  the discrete plane  $\mathbb{Z}^2$ . A point  $x \in E$  is defined by  $(x_1, x_2)$  with  $x_i \in \mathbb{Z}$ . Let  $x \in E$ ,  $r \in \mathbb{N}$ , we denote by  $B_r(x)$  the ball of radius  $r$  centered on  $x$ , defined by  $B_r(x) = \{y \in E, d(x, y) \leq r\}$ , where  $d$  is a distance on  $E$ . We denote by  $B_r$  the map which associates to each  $x$  in  $E$  the ball  $B_r(x)$ . The Euclidean distance  $d$  on  $E$  is defined by  $d(x, y) = [(x_1 - y_1)^2 + (x_2 - y_2)^2]^{1/2}$ . Unless explicitly stated, the choice of the Euclidean distance will be assumed.

An operator on  $E$  is a mapping from  $\mathcal{P}(E)$  into  $\mathcal{P}(E)$ , where  $\mathcal{P}(E)$  denotes the set of all the subsets of  $E$ . Let  $r$  be an integer, the dilation by  $B_r$  is the operator  $\delta_r$  defined by:  $\forall X \in \mathcal{P}(E), \delta_r(X) = \bigcup_{x \in X} B_r(x)$ . The ball  $B_r$  is termed as the structuring element of the dilation. For any operator  $\alpha$ , we define the dual operator  $*\alpha$  by:  $\forall X \in \mathcal{P}(E), *\alpha(X) = \overline{\alpha(\overline{X})}$ , where  $\overline{X}$  denotes the complementary set of  $X$  in  $E$ .

The erosion by  $B_r$  is the operator  $\varepsilon_r$  defined by duality:  $\varepsilon_r = *\delta_r$ . The opening by  $B_r$  is defined by  $\gamma_r = \delta_r \circ \varepsilon_r$ , and the closing by  $B_r$  is defined by  $\phi_r = \varepsilon_r \circ \delta_r$ . Notice that opening and closing are dual to each other, like erosion and dilation. It is well known that for any  $r$ , the opening operator  $\gamma_r$  is increasing ( $\forall X, Y$  subsets of  $E, X \subseteq Y \Rightarrow \gamma_r(X) \subseteq \gamma_r(Y)$ ), anti-extensive ( $\forall X \subseteq E, \gamma_r(X) \subseteq X$ ), and idempotent ( $\forall X \subseteq E, \gamma_r(\gamma_r(X)) = \gamma_r(X)$ ). Also, the closing operator  $\phi_r$  is increasing, extensive ( $\forall X \subseteq E, X \subseteq \phi_r(X)$ ), and idempotent.

Let us now recall the notion of medial axis (see also<sup>17,18</sup>). Let  $X \subseteq E, x \in X, r \in \mathbb{N}$ . A ball  $B_r(x) \subseteq X$  is maximal for  $X$  if it is not strictly included in any other ball included in  $X$ . The medial axis of  $X$ , denoted by  $MA(X)$ , is the set of the centers of all the maximal balls for  $X$  (see Fig. 4e).

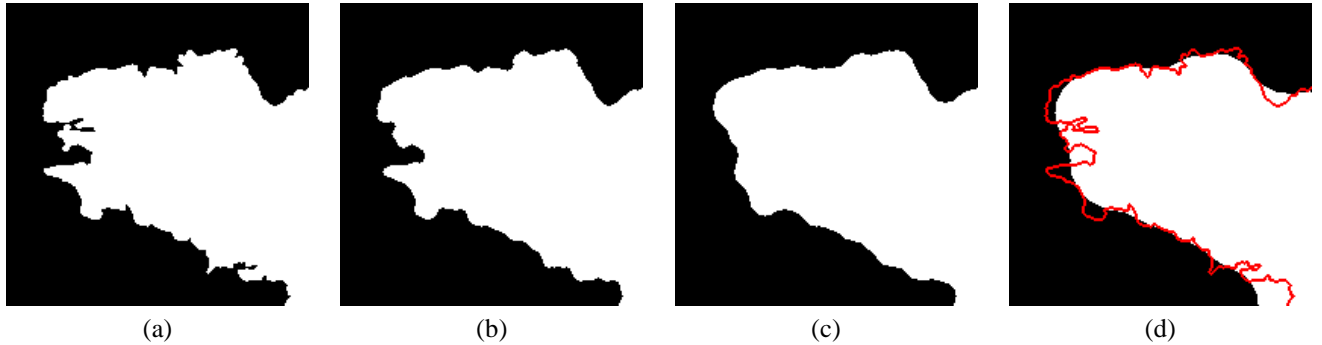


**Figure 1.** (a): a set  $X$ ; (b):  $ASF_3(X)$ ; (c):  $ASF_9(X)$ ; (d): the contour of  $X$ , superimposed to  $ASF_{25}(X)$ .

Alternating sequential filters were introduced by Sternberg<sup>14</sup> and were extensively studied by Serra.<sup>15</sup> Although these filters are useful both for binary and greyscale images, we limit our presentation to the binary case for simplicity. An alternating sequential filter is a composition of openings and closings by balls of increasing radius:

$$ASF_n = \phi_n \circ \gamma_n \circ \phi_{n-1} \circ \gamma_{n-1} \circ \dots \circ \phi_1 \circ \gamma_1$$

As illustrated in Fig. 1, an alternating sequential filter can be used to smooth the contour of an object. Fig. 1d shows  $ASF_{25}(X)$  superimposed to the contour of the set  $X$  given in Fig. 1a. We can notice that  $ASF_{25}(X)$  is neither a superset nor a subset of  $X$ .

In most cases, applying the same alternating sequential filter to the complementary of the object would give approximately\* the same result (up to the complementation). But in some particular cases, the results of  $\text{ASF}_n$  and those of its dual  $*\text{ASF}_n$  can be very different, see Fig. 2. This problem occurs when the object and the background are imbricated together and have the same thickness. This kind of configuration may appear in certain real-world images, such as binarized fingerprint images.

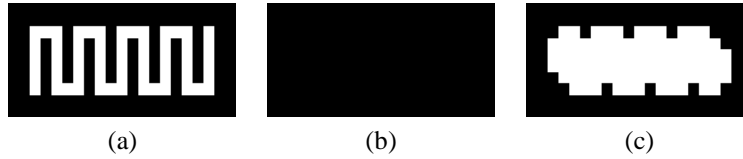


**Figure 2.** (a): a set  $X$  (the line is one pixel thick); (b):  $\text{ASF}_1(X)$ ; (c):  $*\text{ASF}_1(X)$ .

In many applications we need to smooth an object while preserving its topology. In such a case, the alternating sequential filter does not provide satisfactory results, as illustrated in Fig. 3. Also, it may be noticed that the result of an alternating sequential filter  $\text{ASF}_n$  may change dramatically for a small variation of the parameter  $n$  (for example, Great Britain suddenly vanishes from the Europe map between  $n = 22$  and  $n = 23$ ).

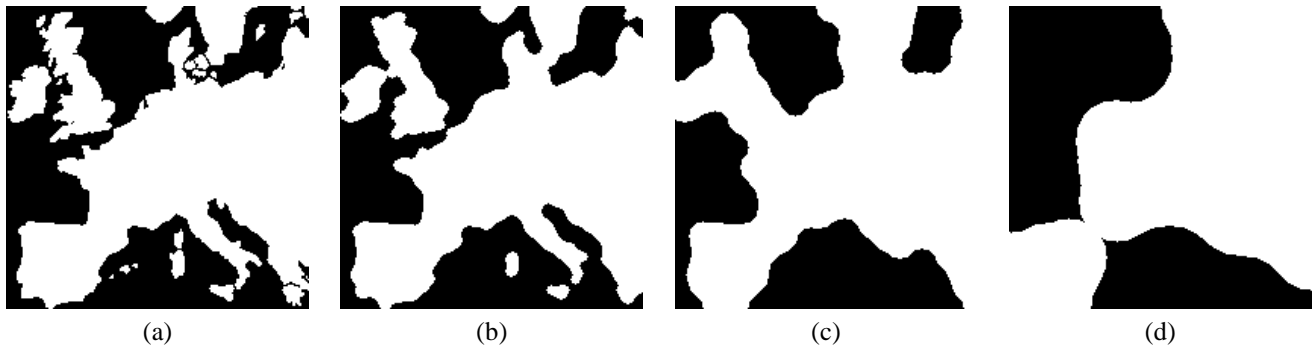


**Figure 3.** (a): a set  $X$ ; (b):  $\text{ASF}_3(X)$ ; (c):  $\text{ASF}_9(X)$ ; (d):  $\text{ASF}_{25}(X)$ . Notice the changes in the number of connected components of both  $X$  and  $\bar{X}$ .

### 3. BASIC NOTIONS OF DIGITAL TOPOLOGY

In this section, we recall some basic notions of digital topology for binary images.<sup>13</sup> For the sake of simplicity, we limit this presentation to the 2D case. We consider the two neighborhoods relations  $\Gamma_4$  and  $\Gamma_8$  defined by, for each point  $x \in E$ :  $\Gamma_4(x) = \{y \in E; |y_1 - x_1| + |y_2 - x_2| \leq 1\}$ ,  $\Gamma_8(x) = \{y \in E; \max(|y_1 - x_1|, |y_2 - x_2|) \leq 1\}$ . In the following, we will denote by  $n$  a number such that  $n = 4$  or  $n = 8$ . We define  $\Gamma_n^*(x) = \Gamma_n(x) \setminus \{x\}$ . The point  $y \in E$  is  $n$ -adjacent to  $x \in E$  if  $y \in \Gamma_n^*(x)$ . An  $n$ -path is a sequence of points  $x_0 \dots x_k$  with  $x_i$   $n$ -adjacent to  $x_{i-1}$  for  $i = 1 \dots k$ .

We say that two points  $x, y$  of  $X$  are  $n$ -connected in  $X$  if there is an  $n$ -path in  $X$  between these two points. This defines an equivalence relation. The equivalence classes for this relation are the  $n$ -connected components of  $X$ , or  $n$ -components in short. A subset  $X$  of  $E$  is said to be  $n$ -connected if it consists of exactly one  $n$ -connected component. The set composed of all  $n$ -connected components of  $X$  which are  $n$ -adjacent to a point  $x$  is denoted by  $C_n[x, X]$ .

In order to have a correspondence between the topology of  $X$  and the topology of  $\bar{X}$ , we have to consider two different kinds of adjacency for  $X$  and  $\bar{X}$ <sup>13</sup>: if we use the  $n$ -adjacency for  $X$ , we must use the  $\bar{n}$ -adjacency for  $\bar{X}$ , with  $(n, \bar{n}) = (8, 4)$  or  $(4, 8)$ . For the sake of simplicity, we assume in the sequel that an adjacency pair has been chosen (e.g.  $(n, \bar{n}) = (8, 4)$ ) and we do not write the subscript  $n$  unless necessary.

Informally, a simple point  $p$  of a discrete object  $X$  is a point which is “inessential” to the topology of  $X$ . In other words, we can remove the point  $p$  from  $X$  without “changing the topology of  $X$ ”. The notion of simple point is fundamental to the

\*In fact the dual of the operator  $\text{ASF}_n$  is not equal to  $\text{ASF}_n$  itself, but to  $\gamma_n \circ \phi_n \circ \gamma_{n-1} \circ \phi_{n-1} \circ \dots \circ \gamma_1 \circ \phi_1$ .

definition of topology-preserving transformations in discrete spaces. We give below a definition and a local characterization of simple points in  $E = \mathbb{Z}^2$ .

The point  $x \in X$  is *simple (for X)* if each  $n$ -component of  $X$  contains exactly one  $n$ -component of  $X \setminus \{x\}$  and if each  $\bar{n}$ -component of  $\bar{X} \cup \{x\}$  contains exactly one  $\bar{n}$ -component of  $\bar{X}$ . Let  $X \subseteq E$  and  $x \in E$ , the two *connectivity numbers* are defined as follows ( $\#X$  stands for the cardinality of  $X$ ):

$$T(x, X) = \#C_n[x, \Gamma_8^*(x) \cap X]; \bar{T}(x, X) = \#C_{\bar{n}}[x, \Gamma_8^*(x) \cap \bar{X}].$$

The following property allows us to locally characterize simple points,<sup>13,19</sup> hence to implement efficiently topology preserving operators:

$$x \in E \text{ is simple for } X \subseteq E \Leftrightarrow T(x, X) = 1 \text{ and } \bar{T}(x, X) = 1.$$

Let  $X$  be any finite subset of  $E$ . The subset  $Y$  of  $E$  is *lower homotopic to X* if  $Y = X$  or if  $Y$  may be obtained from  $X$  by iterative deletion of simple points (see Fig. 4a-b). The set  $Y$  is *upper homotopic to X* if  $\bar{Y}$  is lower homotopic to  $\bar{X}$ , in other words, there is a duality between lower and upper homotopy (see Fig. 4c).

Let  $X$  be any finite subset of  $E$ . We say that a subset  $Y$  of  $X$  is a *homotopic ultimate skeleton of X* if  $Y$  is lower homotopic to  $X$  and if there is no simple point for  $Y$  (see Fig. 4d). Let  $X$  be any finite subset of  $E$ , and let  $C$  be a subset of  $X$ . We say that  $Y$  is a *homotopic ultimate skeleton of X constrained by C* if  $C \subseteq Y$ , if  $Y$  is lower homotopic to  $X$  and if there is no simple point for  $Y$  in  $Y \setminus C$  (see e.g.<sup>20,21</sup>). The set  $C$  is called the *constraint set* relative to this skeleton. A particularly useful constraint set is the medial axis of  $X$ . A homotopic ultimate skeleton of  $X$  constrained by its medial axis is called a *centered skeleton of X*. (see Fig. 4e-f).

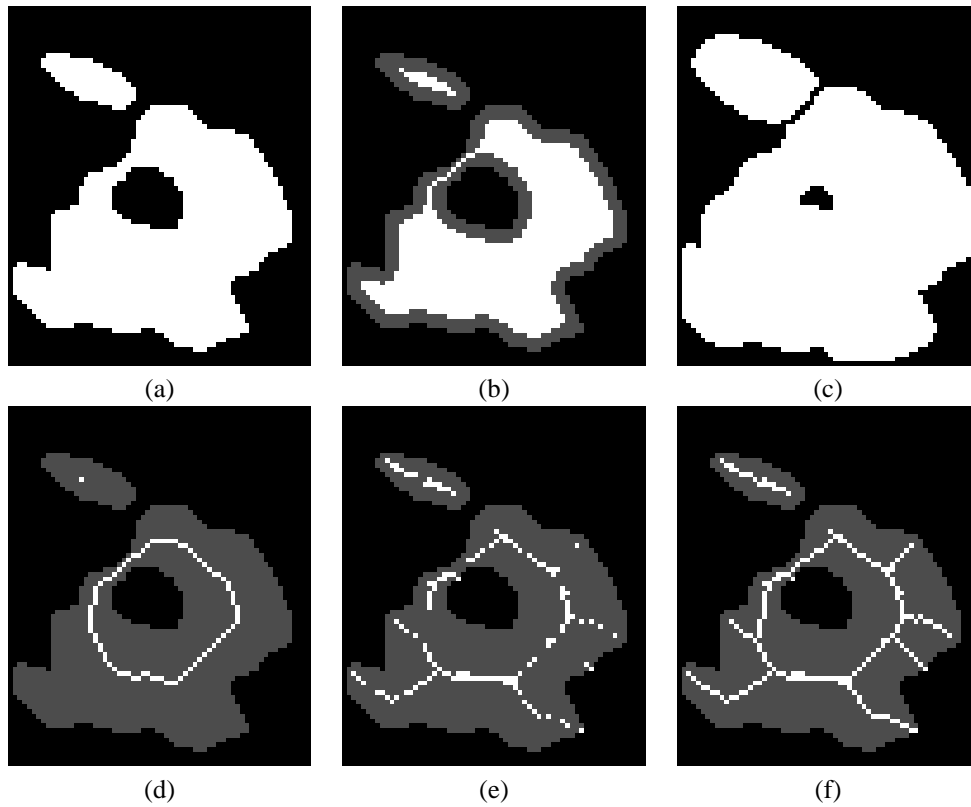


**Figure 4.** (a): a set  $X$  (in white); (b): a set which is lower homotopic to  $X$ ; (c): a set which is upper homotopic to  $X$ ; (d): a homotopic ultimate skeleton of  $X$ ; (e): medial axis of  $X$ ; (f): centered skeleton of  $X$ . In (b,d,e,f) the original set  $X$  appears in dark gray for comparison.

Clearly, there may exist several different ultimate skeletons for a same set  $X$ , depending on the order in which simple points are selected. Several strategies have been proposed to compute homotopic skeletons which are well centered with respect to the original object, see<sup>22</sup> for a survey. We will denote by  $H(X, C)$  a homotopic ultimate skeleton of  $X$  constrained by  $C$  obtained by

following one of these strategies, and we will call *homotopic constrained thinning* this operator  $H$ . For the illustrations of this paper, we choose a strategy which consists in selecting simple points in increasing order of their distance to the background, thanks to a pre-computed quasi-Euclidean distance map.<sup>23</sup>

By duality, we also define the operator  $*H$ , called *homotopic constrained thickening*, as follows: for any finite subset  $X$  of  $E$ , and for any finite superset  $C$  of  $X$ ,  $*H(X, C) = \overline{H(\overline{X}, \overline{C})}$ . This operator thickens the set  $X$  by iterative addition of points which are simple for  $\overline{X}$  and which belong to the set  $C$ , until stability.

#### 4. TOPOLOGICALLY CONTROLLED OPERATORS

Our goal is to propose a smoothing filter which: (i) preserves topology, (ii) preserves the main geometrical features of the object, (iii) has a parameter specifying the “smoothness” of the result, (iv) has a continuous behaviour with regard to this parameter, and (v) smoothes the object and its complementary in an equilibrated way. To achieve these goals, we will combine morphological operators, which provide the desired smoothing effect, and homotopic transformations, which guarantee topology preservation. In this section, we focus on the requirements (i), (ii) and (iii). Requirements (iv) and (v) will be considered in section 5. The requirement (i) will be achieved by the use of the previously introduced homotopic operator  $H$  (and its dual  $*H$ ). The compliance to requirement (ii) and the smoothing effect will be obtained by constraining the homotopic operators by morphological dilations and erosions. The size of the structuring element (i.e. the radius of the ball) for these morphological operators will allow to fulfil requirement (iii).

Let us first consider a “homotopic equivalent” of the erosion, i.e. an operator which shrinks an object while preserving its topology. Such an operator may be defined as a particular case of the homotopic constrained thinning  $H$ , taking as constraint set the erosion of the original object  $X$  by a ball  $B_r$  (see Fig. 5). We obtain a result which is homotopic to the original object, and which has been shrunk according to the size parameter  $r$  (when not in contradiction with topology preservation).

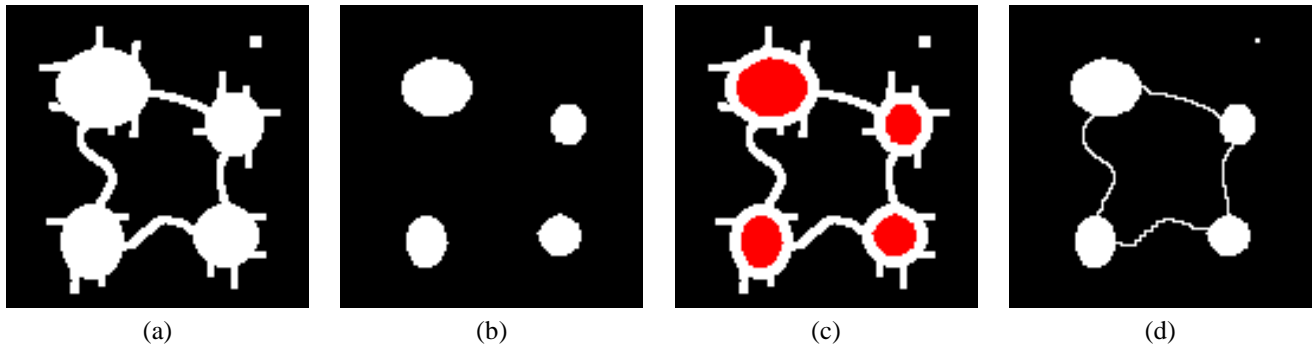


**Figure 5.** (a): a set  $X$ ; (b):  $\varepsilon_5(X)$ ; (c):  $\varepsilon_5(X)$  superimposed to  $X$ ; (d):  $H(X, \varepsilon_5(X))$ .

Like the erosion, this operation is anti-extensive, but it is not increasing, as shown by Fig. 6.

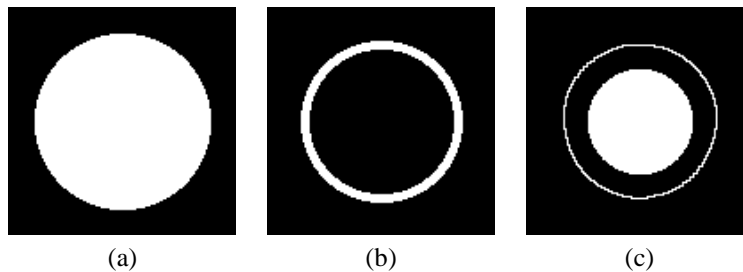


**Figure 6.** (a): a set  $X$ ; (b): a set  $Y \subseteq X$ ; (c): the union of  $H(X, \varepsilon_{20}(X))$  and  $H(Y, \varepsilon_{20}(Y))$ . We see that  $H(Y, \varepsilon_{20}(Y))$  is not included in  $H(X, \varepsilon_{20}(X))$ .

Now suppose we want to have a “homotopic equivalent” of the opening operator. The opening operator consists in an erosion followed by a dilation of the same size. This dilation has the effect of “reconstructing” some parts of the object which

have not been completely deleted by the erosion. If we want to obtain a homotopic operator similar to the opening, several choices may be considered. First, we could use the opening of the original set as a constraint for the operator  $H$ . Fig. 7b shows the drawback of this approach: the parts of the result that have been kept in order to fulfill the topological preservation requirement are not properly reconstructed, they consist of thin lines or isolated points. Intuitively, for such an operator, we want any shape element to be either completely deleted or completely preserved. A second idea is to apply the thickening operator  $*H$  after the application of the thinning operator  $H$ . We see in Fig 7(c) that the result is not satisfactory: the resulting operator is not anti-extensive, contrary to the opening.

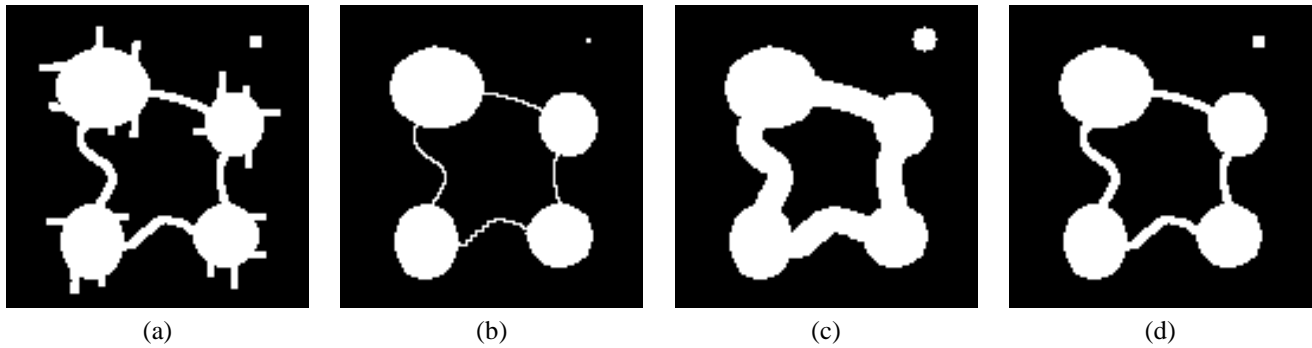


**Figure 7.** (a): a set  $X$  (same as in Fig. 5); (b):  $H(X, \delta_{20}(\epsilon_{20}(X)))$ ; (c):  $*H(Y, \delta_{20}(Y))$ , where  $Y = H(X, \epsilon_{20}(X))$ ; (d):  $*H(Y, \delta_{20}(Y) \cap X)$ , where  $Y = H(X, \epsilon_{20}(X))$ .

To ensure both the anti-extensivity and the preservation of the parts that survive the thinning, it is then natural to take the result of the homotopic thinning  $H(X, \epsilon_r(X))$  (Fig. 5d), to apply a simple dilation (the result on this object would be the same as Fig. 7c), to make the intersection with  $X$  and use this as a constraint for the homotopic thickening of  $H(X, \epsilon_r(X))$  (see the result in Fig. 7d). We give below a more formal definition of this new operator and its dual version.

Let  $X$  be any finite subset of  $E$ , let  $r \in \mathbb{N}$ . The *homotopic cutting of  $X$  by  $B_r$* , denoted by  $HC_r(X)$ , and the *homotopic filling of  $X$  by  $B_r$* , denoted by  $HF_r(X)$ , are defined as follows:  
 $HC_r(X) = *H(Y, \delta_r(Y) \cap X)$ , where  $Y = H(X, \epsilon_r(X))$  ;  
 $HF_r(X) = H(Z, \epsilon_r(Z) \cup X)$ , where  $Z = *H(X, \delta_r(X))$  .  
We can easily see that for any  $r$ ,  $HC_r$  is anti-extensive and  $HF_r$  is extensive.

Figures 7d and 8 illustrate these operators. We can see that the homotopic cutting deletes small capes and the homotopic filling deletes small bays. On the other hand, these operators preserve isthmuses and straits, as well as islands and lakes, which would be deleted by the classical opening and closing. To summarize, the homotopic cutting has a filtering effect similar to the opening, except that thin parts of the object which are necessary for the preservation of topology are left unchanged.

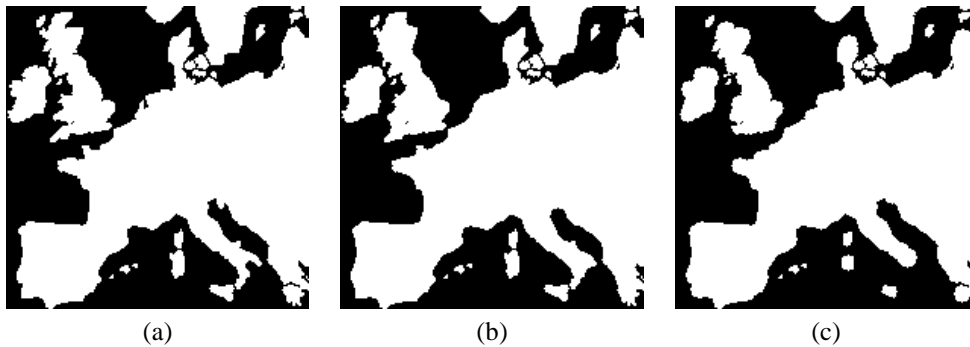


**Figure 8.** (a): a set  $X$ ; (b): homotopic filling  $HF_5(X)$ ; (c): homotopic cutting  $HC_5(X)$ . The homotopic cutting deletes small capes and the homotopic filling deletes small bays. On the other hand, these operators preserve isthmuses and straits, as well as islands and lakes.

We introduce now constrained versions of the homotopic cutting and filling operators, where constraint sets are used to indicate which bays or capes must be preserved, even if their size is small with respect to the parameter  $r$ . We will see in the next section how to use these constraint sets.

Let  $X$  be any finite subset of  $E$ , let  $C \subseteq X, D \subseteq \bar{X}, r \in \mathbb{N}$ . The *homotopic cutting of  $X$  by  $B_r$  with constraint set  $C$* , denoted by  $\text{HC}_r^C(X)$ , and the *homotopic filling of  $X$  by  $B_r$  with constraint set  $D$* , denoted by  $\text{HF}_r^D(X)$ , are defined as follows:  
 $\text{HC}_r^C(X) = *H(Y, \delta_r(Y) \cap X)$ , where  $Y = H(X, \varepsilon_r(X) \cup C)$  ;  
 $\text{HF}_r^D(X) = H(Z, \varepsilon_r(Z) \cup X)$ , where  $Z = *H(X, \delta_r(X) \cap \bar{D})$  .

## 5. HOMOTOPIC ALTERNATING SEQUENTIAL FILTER

In this section, we introduce the homotopic alternating sequential filter (HASF) which is a composition of constrained homotopic cuttings and fillings by balls of increasing radius. It is easy to see that neither homotopic cutting nor homotopic filling are continuous wrt. their numerical parameter (of course, this is also true for opening and closing). This can be highlighted by the following example: take a ribbon of uniform width and apply the operator  $\text{HC}_r$  for increasing values of  $r$ . When  $r$  reaches the width of the ribbon, the result suddenly changes from a ribbon-like shape to a disk-like shape. In order to obtain a smoothing operator which is continuous wrt. its parameter, we control the homotopic alternating sequential filter by two constraint sets  $C$  and  $D$ .

Let  $X$  be any finite subset of  $E$ , let  $C \subseteq X, D \subseteq \bar{X}$ . The *homotopic alternating sequential filter of order  $n$  with constraint sets  $C, D$*  is defined as follows:

$$\text{HASF}_n^{C,D} = \text{HF}_n^D \circ \text{HC}_n^C \circ \text{HF}_{n-1}^D \circ \text{HC}_{n-1}^C \circ \dots \circ \text{HF}_1^D \circ \text{HC}_1^C$$

Notice that if the order  $n$  is greater or equal to the radius of the largest disc which can fit in the object or in the background, then we have  $\text{HASF}_n^{C,D} = \text{HASF}_{n+1}^{C,D} = \text{HASF}_\infty^{C,D}$ .

The idea is to use centered skeletons of the object and of the background as constraint sets (see Fig. 9c), and to smooth the image “as much as possible” using the homotopic alternating sequential filter. Thus, the order of the alternating filter is no more a useful parameter. Instead, we introduce a new parameter which allows to control the shrinking of the constraint sets, hence the degree of smoothing.

Let us consider centered skeletons of  $X$  and  $\bar{X}$  (i.e. homotopic skeletons constrained by the medial axes). By iteratively removing ( $n$  times) extremity points from these skeletons, we obtain a family of constraint sets which “vary smoothly” with respect to the parameter value  $n$ . We give below a formal definition of this family.

Let  $X \subseteq E$ , we set  $C = H(X, \text{MA}(X))$  and  $D = H(\bar{X}, \text{MA}(\bar{X}) \cup \beta)$ , where  $\beta$  denotes the rectangular border of the image domain, and where  $H$  is the homotopic ultimate skeleton defined in section 4. Thus,  $C$  is homotopic to  $X$  and contains  $\text{MA}(X)$ , and  $D$  is homotopic to  $\bar{X}$  and contains  $\text{MA}(\bar{X}) \cup \beta$  (see Fig. 9c). Now we will get our family of constraint sets by successively pruning out extremity points from the sets  $C$  and  $D$ . Let  $\text{SP}(X)$  denote the set of all the points which are simple for  $X$ . We define:

$$C^0 = C ;$$

$$D^0 = D ; \text{ and for } n > 0,$$

$$C^n = H(C^{n-1}, C^{n-1} \setminus \text{SP}(C^{n-1})) ;$$

$$D^n = H(D^{n-1}, D^{n-1} \setminus \text{SP}(D^{n-1})) .$$

In other words,  $C^n$  is obtained from  $C^{n-1}$  by deleting sequentially simple points chosen in the set  $\text{SP}(C^{n-1})$ , until stability (idem for  $D^n$ ). Fig. 10a-c shows the resulting sets (in black for  $C^n$ , in white for  $D^n$ ) for  $n = 10, 30, 60$  respectively.

Using the sets of this family as constraints for the conditional homotopic alternating filter, we obtain the operator which associates, to any subset  $X$  of  $E$  and to any integer  $n$ , the set  $\text{HASF}_\infty^{C^n, D^n}(X)$ , where the families  $\{C^n\}$  and  $\{D^n\}$  are defined as above.

In Fig. 10a-c the contours of the resulting smoothed shapes, as well as the corresponding constraint sets, are superimposed to the original shapes.

This smoothing operator has all the desired properties: it preserves topology, it has a single parameter that controls the smoothing degree, it operates both on the object and on the background in a equilibrated way, and the result of this operator presents small variations in response to small variations of the parameter value.

Notice that, similarly to the morphological alternating sequential filter, the results of this operator and its dual may be quite different on particular shapes. This will be the case, for example, with the shape of Fig. 2, and with a high value  $n$  for the parameter (such that  $C^n$  is reduced to one point and  $D^n$  is equal to  $\beta$ ).

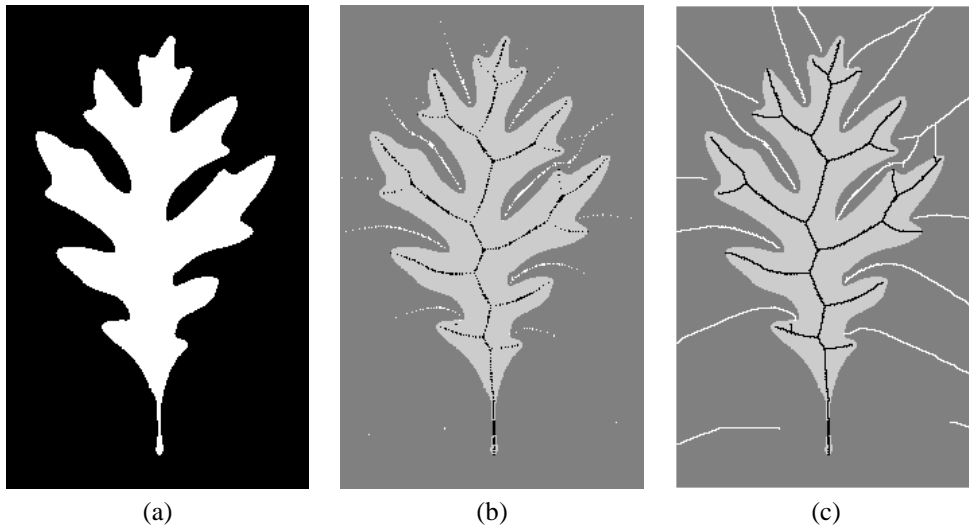


**Figure 9.** (a): a set  $X$ ; (b):  $MA(X)$  (in black) and  $MA(\bar{X})$  (in white); (c):  $C$  (in black) and  $D$  (in white).

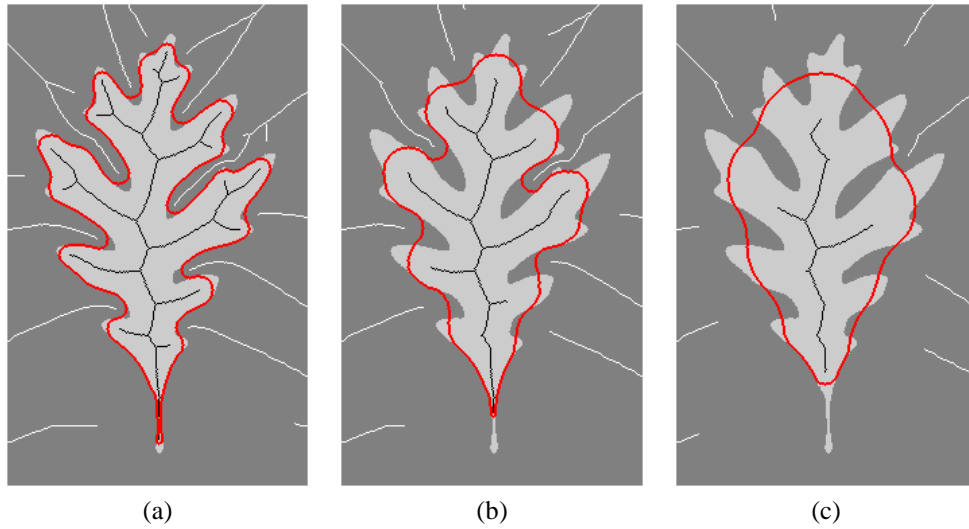


**Figure 10.** (a):  $C^{10}$  (in black) and  $D^{10}$  (in white); contour of  $HASF_{\infty}^{C^{10}, D^{10}}(X)$ ; (b):  $C^{30}$  (in black) and  $D^{30}$  (in white); contour of  $HASF_{\infty}^{C^{30}, D^{30}}(X)$ ; (c):  $C^{60}$  (in black) and  $D^{60}$  (in white); contour of  $HASF_{\infty}^{C^{60}, D^{60}}(X)$ .

## 6. SMOOTHING OF ZOOMED IMAGES

In this section, we present a method based on the homotopic alternating sequential filter for smoothing objects while preserving both topological and geometric features. A very good example of the need for such a method is a binary image which has been zoomed by pixel replication. As we have seen in the introduction, existing methods do not guarantee topology preservation, on the other hand our visual system is very sensitive to the topological characteristics of an image.

Let us consider the image in Fig. 11b, which is a binarization of a pipe smoking man's face (a). This image has been zoomed by a factor 4 in each dimension (c). We will denote by  $X$  the set of white points of this zoomed image. With the aim of smoothing the crenelated contours of the zoomed image, let us first try a simple convolution by a Gaussian kernel followed by a threshold (Fig. 11f). We can observe that some edges are still irregular, while some thin details, both in black and white parts, have disappeared.

Now let us apply the homotopic alternating sequential filter with some adapted constraint sets. Here, we will use medial axes based on the chessboard distance, also called  $d_8$ , which is defined by:  $d_8(x, y) = \max(|x_1 - y_1|, |x_2 - y_2|)$ , where  $x_i$  and  $y_i$



( $i \in \{1, 2\}$ ) denote the coordinates of the points  $x$  and  $y$  of  $E$ . The reason for this choice is explained in the next paragraph. Fig. 11d-e illustrates medial axes obtained using the Euclidean and the chessboard distance, respectively. In the sequel,  $\text{MA}_8(X)$  will be used to denote the medial axis based on the chessboard distance  $d_8$ .

In this application, it makes sense to take as constraint sets the medial axes based on the chessboard distance: the balls for the chessboard distance are squares, and the zoomed image is precisely a union of squares with a minimal side length of four pixels. To preserve the main geometric features of the image, it is sufficient to preserve the centers of maximal squares included in the object and in the background. The use of two different distances is a logical choice with respect to the application: the chessboard distance is best adapted to the description of the original shape, while the Euclidean distance involved in the definition of the homotopic filter is necessary to produce smooth contours in the result.

We set  $C = \text{MA}_8(X)$  and  $D = \text{MA}_8(\bar{X})$ , and we compute  $\text{HASF}_\infty^{C,D}(X)$ . The result is shown in Fig. 11g. It has been obtained in 10 s. on a standard PC, for an image size of  $372 \times 520$ . We get a smooth image with no artefacts, a good preservation of shape, and by construction the preservation of topology is guaranteed. Furthermore, this method has no parameter.

All the operators described in this paper can be easily extended to the 3D discrete grid  $\mathbb{Z}^3$ . In fact these operators only involve only morphological operators which can be extended to  $\mathbb{Z}^3$  in a straightforward manner, and the notion of simple point, which has also an efficient characterization in the 3D cubic grid.<sup>19</sup> To conclude this section, we show an application on a zoomed 3D binary image.

The image in Fig. 12b is a rendering of the left ventricle of a human heart. The original 3D image has been obtained from a MRI device. We have segmented 10 sections (2D images) extracted from the DICOM<sup>†</sup> file, and we simply stacked the results (Fig. 12a). The dimensions of the pixel in each section ( $x, y$  axes) are  $1.5\text{mm} \times 1.5\text{mm}$ , and the distance between two sections ( $z$  axis) is 6mm. To get the object shown in Fig. 12b, each  $xy$  section has been replicated four times in order to obtain a more realistic visualization (we will denote this object by  $X$ ). Fig. 12c shows a rendering of  $\text{HASF}_\infty^{C,D}(X)$ , where  $C = \text{MA}_{26}(X)$ ,  $D = \text{MA}_{26}(\bar{X})$ , and where  $\text{MA}_{26}$  denotes the medial axis based on the distance  $d_{26}$  defined by:  $d_{26}(x, y) = \max(|x_1 - y_1|, |x_2 - y_2|, |x_3 - y_3|)$ . This result has been obtained in 75 s. on a standard PC, for an image size of  $80 \times 80 \times 48$ . In Fig. 12d,e we show different renderings of the 3D objects depicted in Fig. 12b,c respectively. These renderings were obtained by using a topologically sound variant of the ‘‘marching cubes’’ method<sup>24</sup> to obtain a triangulated surface, and by displaying this surface using a ray-tracer. No smoothing was applied to the mesh vertices, only the Phong method<sup>25</sup> was used to interpolate normals.

## 7. CONCLUSION

Topological characteristics are fundamental attributes of an object. In many applications, it is mandatory to preserve or control the topology of an image. Nevertheless, the design of transformations which preserve both topological and geometrical features of images is not an obvious task, especially in 3D. In fact, except for the notable case of homotopic skeletons, few transformations based on these two criteria have been proposed.

In this paper, we introduced the homotopic alternating sequential filter, a general topology-preserving operator with a smoothing effect which is controlled by a constraint set. In contrast with the skeleton transformation, the homotopic alternating sequential filter does not only remove simple points from the object, but also adds some simple points, treating both the object and the background in an equilibrated way. Depending on the chosen constraint set, this operator may be used in different ways. We presented a method without any parameter for smoothing zoomed 2D and 3D images while preserving topology, using medial axes based on a discrete distance as constraint set. We also presented a general topology preserving smoothing method which allows to control the degree of smoothing by a single parameter, such that little variations of the parameter only provoke little variations of the result.

The notions of simple point and homotopic skeleton have been generalized to the case of multilevel (i.e. grayscale) images by G. Bertrand et al.<sup>26</sup> This allows us to extend the smoothing procedures introduced in this paper to the case of multilevel images. This extension will be discussed in forthcoming publications.

**Acknowledgements** The authors wish to thank professors J.L. Dubois-Randé, J. Garot (Hôpital Henri Mondor, Créteil, France) for the heart images.

---

<sup>†</sup>DICOM is a standard format for the storage and exchange of medical data.

## REFERENCES

1. J. Hu, D. Yu, H. Yan: "A multiple point boundary smoothing algorithm", *Pattern Recognition Letters*, Vol. 19, pp. 657-668, 1998.
2. A. Asano, T. Yamashita, S. Yokozeki: "Active contour model based on mathematical morphology", *ICPR 98*, pp. 1455-1457, 1998.
3. F. Leymarie, M.D. Levine: "Curvature morphology", *Proceedings of Vision Interface '89*, pp. 102-109, 1989.
4. S.B. Ho, C.R. Dyer: "Shape smoothing using medial axis properties", *IEEE Trans. on PAMI*, Vol. 8, No. 4, pp. 512-520, 1986.
5. B.K. Jang, R.T. Chin: "Morphological scale space for 2d shape smoothing", *Computer Vision and Image Understanding*, Vol. 70, pp. 121-141, 1998.
6. G. Taubin: "Curve and surface smoothing without shrinkage", *Proceedings of ICCV'95*, pp. 852-857, 1995.
7. J. Vollmer, R. Mencl, H. Müller: "Improved laplacian smoothing of noisy surface meshes", *Proceedings of Computer Graphics Forum (Eurographics '99)*, Vol. 18, No. 3, pp. 131-138, 1999.
8. Y. Ohtake, A.G. Belyaev, I.A. Bogaevski: "Polyhedral surface smoothing with simultaneous mesh regularization", *Proceedings of Geometric Modeling and Processing 2000*, pp. 229-237, 2000.
9. X. Liu, H. Bao, H-Y. Shum, Q. Peng: "A novel constrained smoothing method for meshes", *to appear in Graphical Models*, 2002.
10. B.B. Kimia, K. Siddiqi: "Geometric heat equation and nonlinear diffusion of shapes and images", *Computer Vision and Image Understanding*, Vol. 64, No. 3, pp. 305-322, 1996.
11. L. Moisan: "Affine plane curve evolution: a fully consistent scheme", *IEEE Trans. on Image Processing*, Vol. 7, No. 3, pp. 411-420, 1998.
12. M. Grayson: "The heat equation shrinks embedded plane curves to round points", *J. Differential Geometry*, Vol. 26, pp. 285-314, 1987.
13. T. Yung Kong, A. Rosenfeld: "Digital topology: introduction and survey", *Computer Vision, Graphics and Image Processing*, Vol. 48, pp. 357-393, 1989.
14. S.R. Sternberg, "Grayscale Morphology", *Computer Vision, Graphics, and Image Understanding*, 35, pp. 333-355, 1986.
15. J. Serra, *Image Analysis and Mathematical Morphology, Vol. II: Theoretical Advances*, Chap. 10, Academic Press, 1988.
16. J. Serra, *Image Analysis and Mathematical Morphology*, Academic Press, 1982.
17. A. Rosenfeld, A.C. Kak: *Digital Image Processing*, Academic Press, 1982.
18. H. Talbot, L. Vincent: "Euclidean skeletons and conditional bisectors", *Proceedings of VCIP'92, SPIE*, Vol. 1818, pp. 862-876, 1992.
19. G. Bertrand: "Simple points, topological numbers and geodesic neighborhoods in cubic grids", *Pattern Recognition Letters*, Vol. 15, pp. 1003-1011, 1994.
20. E.R. Davies, A.P.N. Plummer: "Thinning algorithms: a critique and a new methodology", *Pattern Recognition*, Vol. 14, pp. 53-63, 1981.
21. L. Vincent: "Efficient Computation of Various Types of Skeletons", *Proceedings of Medical Imaging V, SPIE*, Vol. 1445, pp. 297-311, 1991.
22. L. Lam, S-W. Lee, C.Y. Suen: "Thinning methodologies - a comprehensive survey", *IEEE PAMI*, Vol. 14, No. 9, pp. 869-885, 1992.
23. P.E. Danielsson: "Euclidean distance mapping", *Computer Graphics and Image Processing*, 14, pp. 227-248, 1980.
24. J.O. Lachaud, A. Montanvert: "Continuous analogs of digital boundaries: a topological approach to iso-surfaces", *Graphical models*, Vol. 62, No. 3, pp. 129-164, 2000.
25. B.T. Phong: "Illumination for computer generated pictures", *Communications of the ACM*, Vol. 18, No. 6, pp. 311-317, 1975.
26. G. Bertrand, J. C. Everat and M. Couprie: "Image segmentation through operators based upon topology", *Journal of Electronic Imaging*, Vol. 6, No. 4, pp. 395-405, 1997.

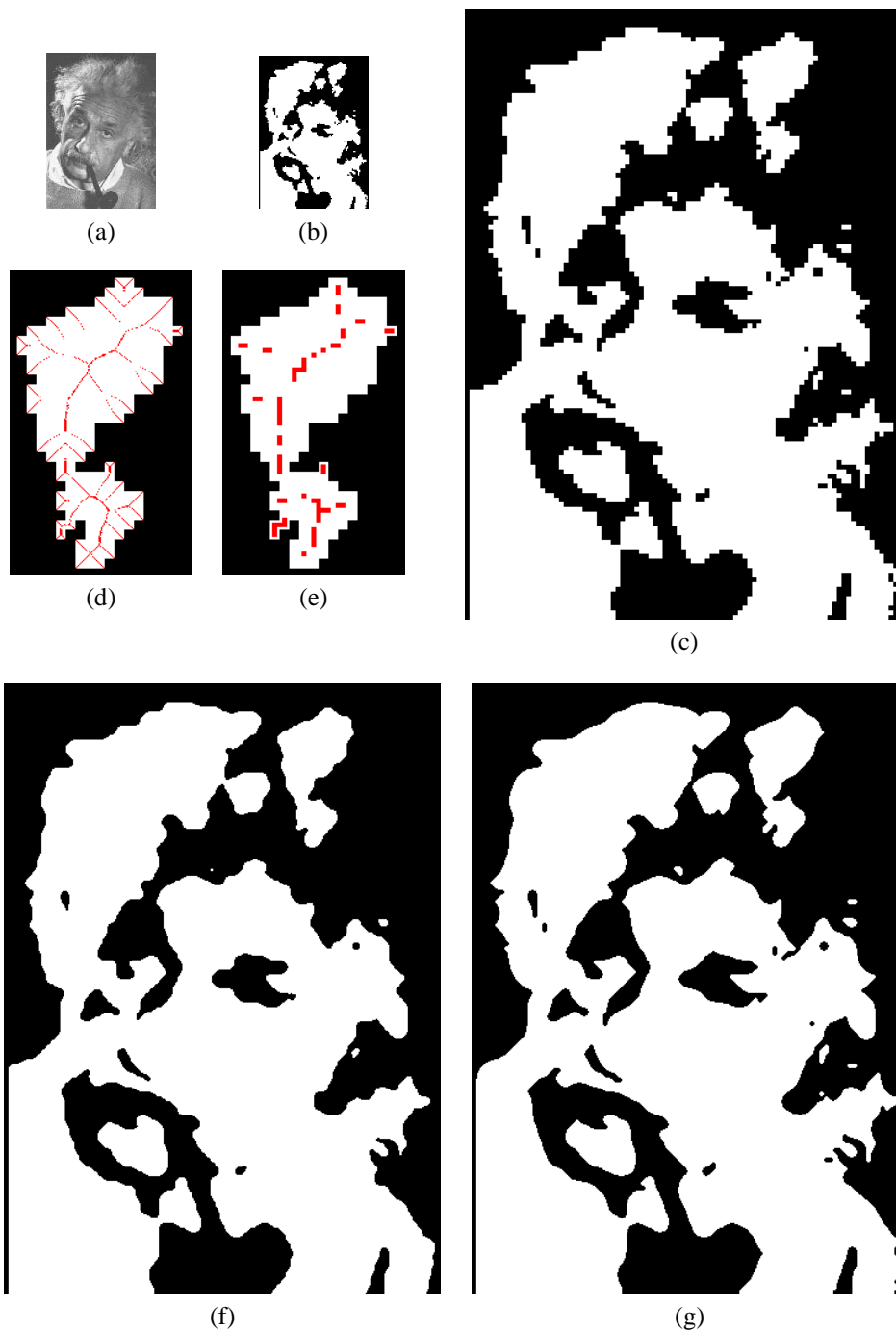
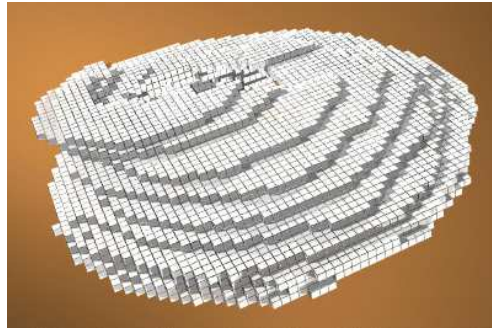
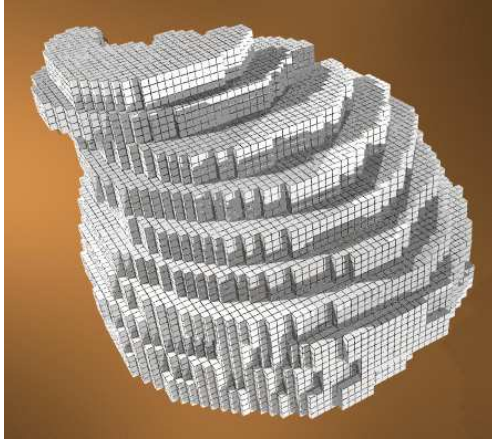


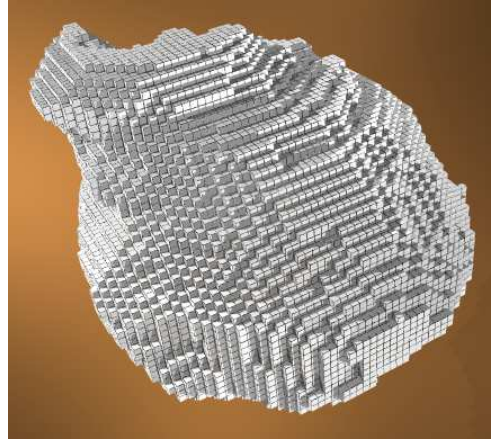
**Figure 11.** (a): a pipe smoking man's face; (b): a binarization of (a); (c): image (b) zoomed 4 times (set  $X$ ); (d): medial axis based on the Euclidean distance; (e): medial axis based on the chessboard distance; (f): threshold of a convolution of  $X$  by a Gaussian kernel; (g):  $\text{HASF}_{\infty}^{C,D}(X)$ , with  $C = \text{MA}_8(X)$  and  $D = \text{MA}_8(\bar{X})$ .



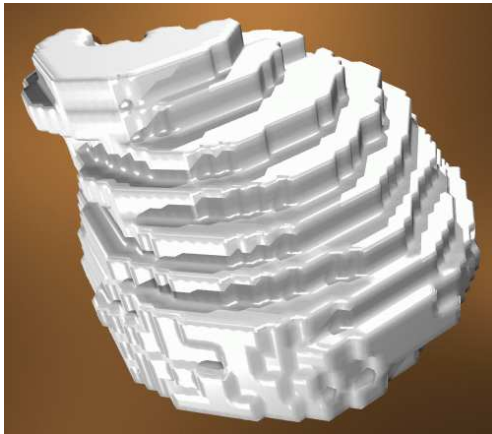
(a)



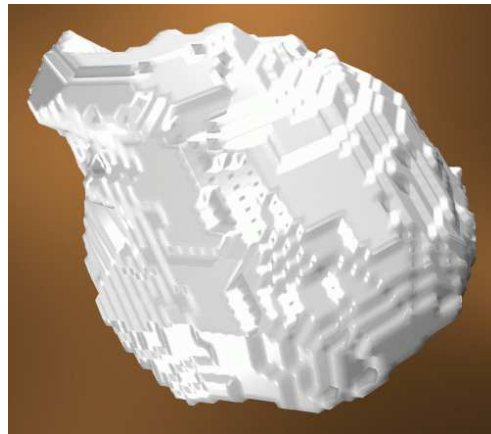
(b)



(c)



(d)



(e)

**Figure 12.** (a): a rendering of a 3D object (slices of the left ventricle of a human heart) ; (b): object  $X$ : the original object zoomed by 4 in the  $z$  direction ; (c): a rendering of  $\text{HASF}_{\infty}^{C,D}(X)$ , with  $C = \text{MA}_{26}(X)$  and  $D = \text{MA}_{26}(\bar{X})$  ; (d): another rendering of the object in (b) ; (e): another rendering of the object in (c).